Electrochimica Acta 426 (2022) 140809

Contents lists available at ScienceDirect

Electrochimica Acta

journal homepage: www.journals.elsevier.com/electrochimica-acta

Influence of the dwell time in the polarization hysteresis of polymer electrolyte membrane fuel cells

Alfredo Iranzo [a,b,*], Sergio J. Navas [b], Javier Pino [a], Numa A. Althubiti [c], Mohamed R. Berber [d,e,**]

[a] Thermal Engineering Group, Energy Engineering Department, School of Engineering, University of Sevilla, Camino de los Descubrimientos s/n, Sevilla 41092, Spain
[b] AICIA – Thermal Engineering Group, Camino de los Descubrimientos s/n, Sevilla 41092, Spain
[c] Physics Department, College of science, Jouf University, Sakaka 2014, Saudi Arabia
[d] Chemistry Department, College of Science, Jouf University, Sakaka 2014, Saudi Arabia
[e] Department of Chemistry, Faculty of Science, Tanta University, Tanta 31527, Egypt

ARTICLE INFO

Keywords:
Fuel cell
Voltage hysteresis
Dwell time
Electrochemical impedance spectroscopy
Equivalent circuit

ABSTRACT

The extent of the cell voltage hysteresis observed in polarization curves of PEM fuel cells and the origins causing this effect are investigated by performing experimental polarization curves with different dwell times for a 50 cm^2 PEM fuel cell. Electrochemical Impedance Spectroscopy measurements are carried out in order to determine the relative contributions of the different polarizations (ohmic, activation, and concentration polarization). Equivalent circuits were obtained from the impedance spectra, where the interpretation of the circuit parameters enabled the analysis of the origin and extent of the cell voltage hysteresis. It was identified that the cause of the cell voltage hysteresis is actually dominated by the changes in the concentration polarization at low current densities, and by the changes in the activation polarization at high current densities. The cell ohmic resistance (and consequently the membrane hydration) presents a minor effect on the cell voltage hysteresis. The effect of the dwell time in the cell voltage hysteresis (with values ranging from 15 to 25 mV) presents a mixed trend, with an initial decrease for increasing dwell times from 120 to 600 s, and a later increase and a final almost constant hysteresis for longer dwell times.

1. Introduction

The observation that fuel cells (FCs) present a voltage hysteresis when performing the polarization curve in the forward direction with increasing currents and then in backward direction with decreasing currents is a well-known effect widely reported in the literature [1–4]. Although it was initially considered that only water flooding was the origin of such effect (cell switching from drier to more flooded conditions or the other way round), it was later recognised that additional and complex phenomena is influencing the cell voltage hysteresis, such as the difference of the membrane humidification levels, and the presence/absence of oxide species adsorbed onto the surface of the catalyst. Mitzel et al. [5] indicated that the hysteresis in the cell voltage of the polarization curves could not actually be avoided, regardless the dwell time used at each test point.

Voltage hysteresis is a relevant phenomenon when the fuel cell is operating under frequent load changes due to variations in the power requirements demanded to the FC system. The transient behaviour of the cell is thus important not only in terms of the dynamic response, but also in terms of the control system design and optimization, where the new operating point after load change may vary due to the hysteresis effect depending on whether the current density is increasing or decreasing. It also generates difficulties when it comes to comparing polarization curves, as hysteresis will appear regardless of the dwell times used in the experiment, set-points defined for the current, or previous load levels (ascending or descending currents). Indeed, Mitzel et al. [5] introduced the concept of "steady-state" polarization curves for a more suitable benchmarking among different cells or stacks, consisting on calculating the average cell voltage (for each current) between the ascending and descending polarization curves in order to obtain a fair polarization

* Corresponding author at: Thermal Engineering Group, Energy Engineering Department, School of Engineering, University of Sevilla, Camino de los Descubrimientos s/n, Sevilla 41092, Spain.
** Corresponding author at: Chemistry Department, College of Science, Jouf University, Sakaka 2014, Saudi Arabia.
E-mail addresses: airanzo@us.es (A. Iranzo), mrberber@ju.edu.sa (M.R. Berber).

https://doi.org/10.1016/j.electacta.2022.140809
Received 16 March 2021; Received in revised form 30 September 2021; Accepted 4 July 2022
Available online 6 July 2022

curve and benchmarking with a minimum influence of hysteresis. This was also included in harmonized test protocols for fuel cells such as the one by the Joint Research Centre of the European Commission [6,7].

Cell hysteresis in polarization curves was also studied by using galvanostatic step sweep by Hou [8] for different Gas Diffusion Layers. The extent of the hysteresis was associated with the capability of the membrane electrode assembly (MEA) and the gas diffusion layer (GDL) to store the water generated by the electrochemical reaction after the load change (the extent of the "water reservoir" as indicated by Hou [8]). In addition, it must be considered that the different processes taking place within the FCs are occurring at significantly different time scales [9,10], which is influencing the dynamic and transient response of the cell. While ohmic response is mostly instantaneous, the electrochemical reactions at the double layer present characteristic timescales of milliseconds. However, the reactants diffusion is a slower process and timescale ranges in the 0.1–1 s [11], and liquid water transport among MEA, GDL and channels may take several seconds and even minutes depending on the cell size [12], when the coupling with heat transfer is considered.

Several experimental techniques are commonly available to better gain more insights into the phenomena that take place within the FC. The cell polarization curve (I-V curve) is representing the performance of a FC, but as it shows the integral output of all phenomena occurring within the cell, and the different individual physical-electrochemical processes cannot be properly determined. In contrast, Electrochemical Impedance Spectroscopy (EIS, or AC impedance spectroscopy) is enabling the analysis and quantification of the different overpotentials or polarization contributions, the determination of catalyst parameters [13] or the monitoring and diagnosis of degradation and state-of-health [14]. The use of EIS for the analysis of the performance of PEMFCs as well as optimization, monitoring, and diagnosis is detailed in the review work by Wu et al. [15], Rezaei Niya and Hoorfar [16], Tang et al. [17], and Yuan et al. [18]. In a representation and quantitative analysis of the impedance spectra obtained, the charge transfer resistance (activation polarization), reactants transport resistance (concentration polarization), or ohmic resistance (also known as HFR o High Frequency Resistance) can be quantified [19]. For a PEMFC operating with air, Nyquist plots typically show two pronounced arcs or semi-circles impedance spectra, the medium frequencies arc (between 10 and 100 Hz) corresponding to charge transfer resistance, and the low frequencies arc (at low frequencies ≈ 1–10 Hz) corresponding to reactant diffusion limitation, usually in the cathode side [15–18].

By combining this technique together with the Distribution of Relaxation Times (DRT) method, the characteristic timescales of the different processes occurring within the PEMFC can also be studied and determined, as in the work by Weiß et al. [20], Heinzmann et al. [21,22] or Iranzo et al. [23]. In this work, the extent of the cell voltage hysteresis and the origins causing this effect are investigated by performing experimental polarization curves with different dwell times, for a 50 cm^2 PEMFC. EIS measurements were carried out in order to determine the different contributions of the polarization curves (ohmic, activation, and mass transport or concentration polarization).

2. Experimental facility and methodology

2.1. Test station and fuel cell description

A PEMFC test station was used for the experimental work, where the main components of the station are an electronic load ADAPTIVE POWER 5L18-24 (0-60V/0-240A), a power source MAGNA POWER SL5-250/UI (0-5V/0-250A), a Frequency Response Analyzer NEWTONS 4th PSM1700, a cell heating/cooling system, and a system to control gas flow, pressure and relative humidity. The sample rate of the station is 1 Hz and its voltage measurement uncertainty ±1 mV.

The PEMFC used is a 50 cm^2 single cell from ElectroChem Inc., with serpentine flow fields in cathode and anode, in a cross-flow layout with horizontal anode and vertical cathode channels as depicted in our previous publications [19,23]. The land width and channel are 0.86 mm and 0.71 mm, respectively. A 5-layer 50 cm^2 MEA was used, with a Nafion-212 membrane, 1.0 mg Pt/cm^2 in the anode and cathode electrodes (with 20 wt% Pt/C). GDLs were from Toray (TP-060 without MPL), 0.19 mm thick and 78% porosity, with an electrical resistivity of 80 mΩcm^2.

2.2. Experimental conditions

The operating conditions of the fuel cell were defined as following. Reactants relative humidity of 60%, stoichiometric factors at the anode and cathode 1.3 and 2.5, respectively, cell temperature of 65 °C, and cell pressure 0.5 bar (relative). The oxidant used was air. All the experiments carried out to obtain the different I-V polarization curves at different dwell times (120–1800 s) were performed at the same nominal conditions, which are the same as proposed in Iranzo et al. [23]. The cell temperature was maintained constant at 65 °C during all experiments, in order to avoid temperature effects on the membrane hydration levels and the consequent variations in the cell resistance. This was achieved by a temperature control system consisting of film heaters on both sides of the cell and air fan coolers also on both sides of the cell, with a thermocouple inserted into the cathode Bipolar Plate to monitor the cell temperature.

2.3. Description of the experimental testing procedure

The experimental procedure used for the assessment of the hysteresis of I-V polarization curves was based on the one defined by the Joint Research Centre of the European Commission [6]. Each of the polarization curves are recorded the initial current density points from 0 to 0.1 A/cm^2 evaluated in steps of 0.02 A/cm^2 with a dwell time of 60 s, with the exception of point at OCV that had a dwell time of 30 s only to prevent electrode degradation. All the rest of the current density points, ranging from 0.2 to 1.3 A/cm^2 for this particular cell and operating conditions, were evaluated in steps of 0.1 A/cm^2 with the dwell time determined for each test. In all cases the forward (increasing current) and backward (decreasing current) polarization curves were recorded in order to evaluate the cell voltage hysteresis. The tests carried out corresponded to dwell times of 120, 200, 600, 900, 1200, and 1800 s. In all cases the data acquisition / sampling rate during the test is 1 Hz.

After the completion of each polarization curve, the voltage corresponding to each current density point was calculated as the average value of the last 30 s measured (resulting in 30 measurements for each point). For each dwell time analysed, a minimum of three curves were measured, and the final polarization curve presented was calculated as the average value.

The EIS impedance measurements were performed with amplitude of 10% of the base intensity and with a frequency range between 0.2 and 6.0 kHz (with over 14 points per decade). Each of these frequency sweeps lasts around 300 s. Therefore, no EIS experiments were carried out for the low dwell times. For the dwell times analysed, the EIS spectra were recorded at 25 and 50 A (0.5 and 1.0 A/cm^2).

3. Results

3.1. Polarization curves

The I-V polarization curves obtained for all the dwell times tested (120–1800 s) are represented in Fig. 1 (top) where a close-up between 60 A and 70 A is included for a better representation of the voltage differences at higher currents (Fig. 1, bottom). Both forward and backward steps are represented. Error bars are included in Fig. 1 (bottom) for a determination of the measurement uncertainty.

It can be observed that all curves are similar, but two distinctive groups are identified at high currents; one presenting higher cell

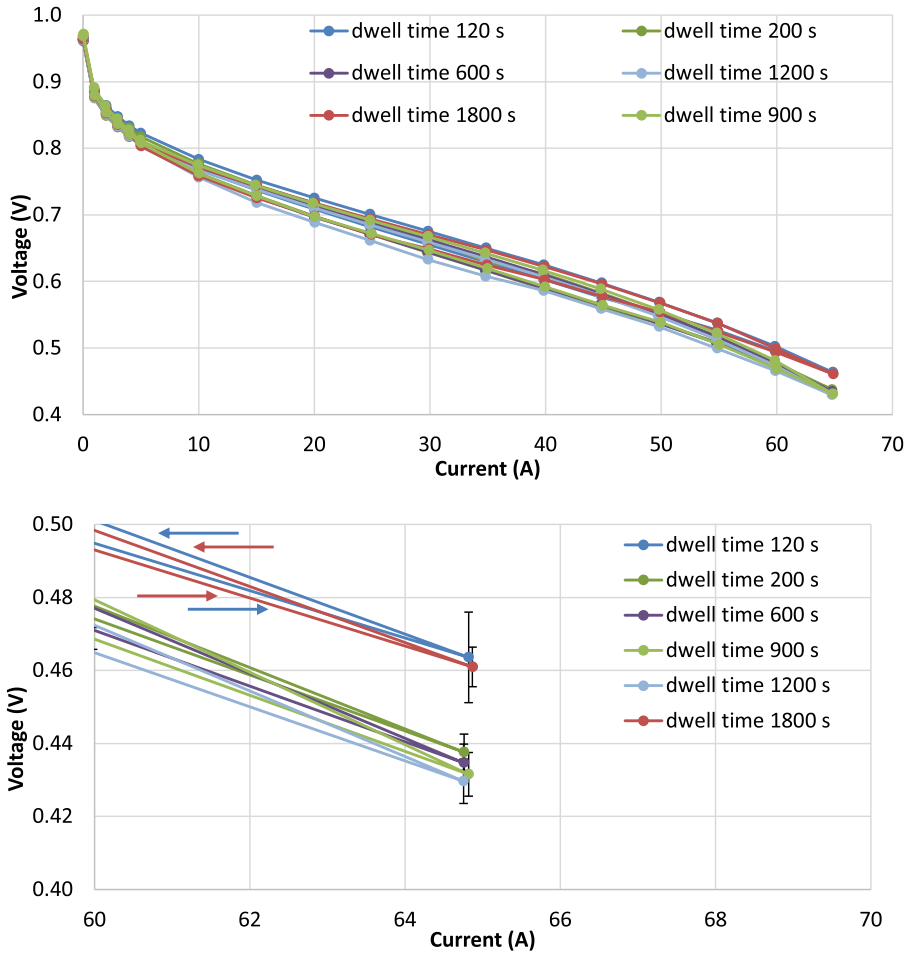

Fig. 1. Polarization curves measured for different dwell times (top). Detail at higher currents (bottom) with error bars marked. Arrows indicate the forward (increasing current) and backward (decreasing current) curves for dwell time 120 s (blue) and 1800 s (red).

voltages (around 0.46 V at 65 A) which corresponds to the minimum and the maximum dwell times (120 and 1800 s), and the rest of the curves with intermediate dwell times presenting lower cell voltages (around 0.43–0.44 V at 65 A). It is also identified that for all dwell times the backward curve corresponding to decreasing currents is above the forward curve, presenting higher cell voltages for all values of the current being drawn from the cell, as marked with arrows in Fig. 1 (bottom).

3.2. *Quantification of the cell voltage hysteresis*

In order to quantify the hysteresis in each polarization curve, two different calculation methods were followed, i.e. hysteresis as the cell voltage difference at a particular current density in the galvanostatic experiment, and hysteresis accounted as the area enclosed among both forward and backward curves, which is indeed the product of ΔV x ΔI (thus with units of power). The results are presented in Fig. 2, where it can be observed that both methods are qualitatively equivalent in terms of the trends followed with respect to the dwell time.

When measured as voltage difference between forward and backward curves for a given current, the hysteresis at 25 A (middle part of the curve in the ohmic region) was the highest, whereas the hysteresis at 10 A (initial part of the curve in the activation region) was the lowest. The effect of the dwell time in the experiment presented a mixed trend. Initially, the hysteresis decreased when the dwell times increased from 120 to 600 s, and then started to increase up to 900 s dwell time, and finally reached a plateau with minor variations until 1800 s. As a global indication, cell voltage hysteresis for the conditions tested is ranging from 15 to 25 mV according to the results presented in Fig. 2, which is consistent with values reported in the literature (e.g. 20 mV reported by Mitzel et al. [5]).

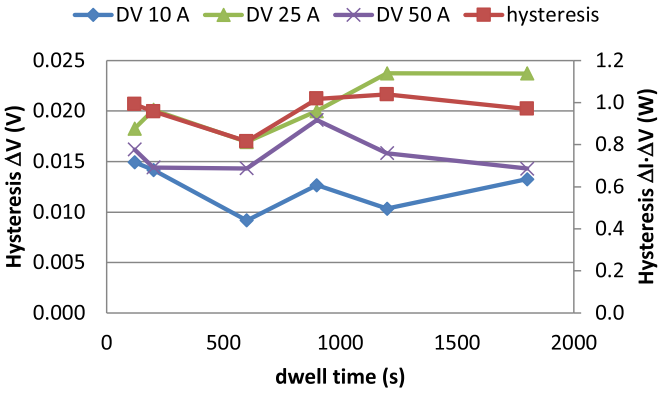

Fig. 2. Hysteresis of the I–V curves measured for the different dwell times.

3.3. *Effect of HFR on the cell voltage hysteresis*

The HFR values were obtained from the EIS experiments at high frequencies and are represented in Fig. 3. The objective is to analyse the eventual effect of the cell resistance on the hysteresis observed. The HFR values were determined from the Nyquist plots as the Z_{Re} value for $Z_{im} = 0$ (typically $Z_{im} = 0$ at 5–6 kHz). The HFR values represented in Fig. 3

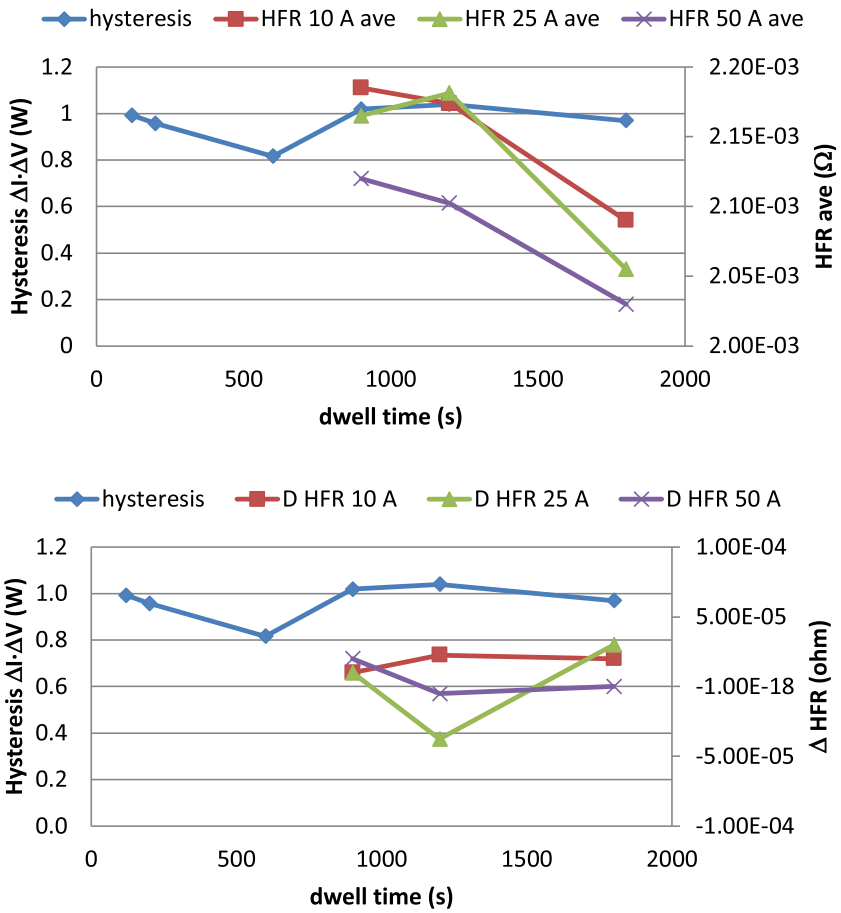

Fig. 3. HFR values measured for the different dwell times at 10 A, 25 A, and 65 A. Average HFR values between forward and backward I–V curves (top). HFR difference between forward and backward I–V curves (bottom).

(top) are actually the average values between the forward and backward curves. In Fig. 3 the HFR values are not available for short dwell times. Although it is possible to obtain HFR values in short testing times, it was intended in this work to obtain complete EIS measurement in all cases, where full EIS spectra was not measured for short dwell times due to the lack of enough testing time to complete the test with enough accuracy. HFR values in Fig. 3 (bottom) are calculated as the difference between the values measured for the forward and backward curves.

The HFR results compare well with results reported in the literature, where a summary of HFR values for different conditions can be found in the review work by Rezai Niya et al. [24].

The following observations are determined from the results obtained. First, HFR values (cell ohmic resistance) are decreasing as the current increases (Fig. 3, top), due the fact that higher amount of water is produced by the electrochemical reaction thus improving the membrane hydration. This is a well-known relationship [1,25]. The HFR variations are however very small, with less than 5% decrease in the absolute value of HFR. In terms of the effect of the dwell time, for the data collected it is observed that HFR values decreases for higher dwell times. In any case, it can be determined that the HFR is not having a significant influence on the voltage hysteresis. The conclusion that the differences in HFR values between the forward and the backward curves are actually not influencing the hysteresis was determined by comparing the voltage difference caused by the HFR difference. Basically, the HFR difference between forward and backward curves is roughly 1.0E-5 Ohm for 10 A, 25 A and 50 A, which implies a voltage difference of 0.1 mV, 0.25 mV, or 0.5 mV, respectively. However, the hysteresis measured as voltage difference between the forward and the backward curves (Fig. 2) is within 15–25 mV, so it is clear that the differences in the HFR values (i.e. differences in membrane hydration) cannot be causing the cell voltage hysteresis observed. This will be further studied and determined with the corresponding resistance values obtained by means of the Equivalent Circuit models in Sections 3.4 and 3.5.

3.4. *Determination of the cell electrochemical and reactant diffusion resistances*

Nyquist plots for the different dwell times where EIS measurements are available are shown in Fig. 4. Measurements were conducted for dwell times 900, 1200, and 1800 s, as smaller dwell times did not allow for an accurate EIS measurement along the full frequency range (6–0.2 Hz).

In all cases the impedance spectra present the well-known two arcs corresponding to the activation polarization (left arc at medium frequencies) and to the mass transport polarization (right arc at lower frequencies) [15–19,23]. Both arcs (or semi-circles) are clearly overlapping for the higher current density operation (1.0 A/cm^2, Fig. 4, bottom). It can be also observed that the arc corresponding to activation overpotential is decreasing for increasing currents, whereas the arc corresponding to mass transport losses is increasing for higher currents. This is an expected behaviour as when the load current increases, the reactants consumption increases simultaneously and requires a higher reactant flux, but the formation of product water at cathode will hinder the oxygen diffusion thus increasing the corresponding polarization resistance and the low-frequency arc in the Nyquist plot.

In order to achieve a quantitative analysis, the impedance spectra were fitted in *Z*View [26] to a well-known Equivalent Circuit composed by a resistance, and a CPE element in parallel with a second resistance

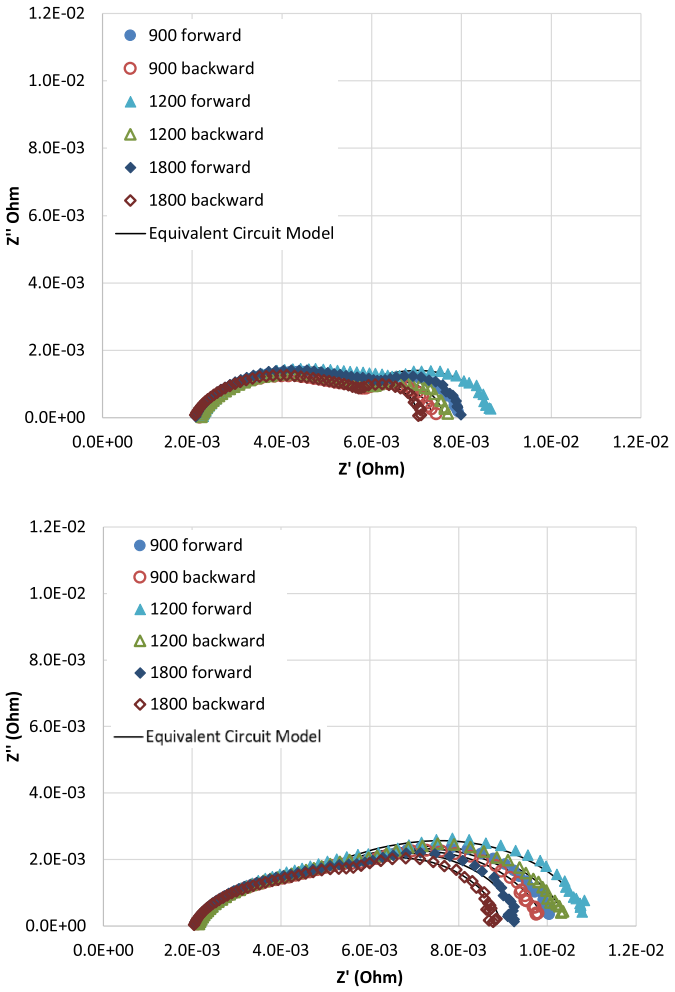

Fig. 4. Nyquist plots obtained from EIS measurements for dwell times 900, 1200, and 1800 s, at 25 A (top) and 50 A (bottom).

and a Warburg element as shown in Fig. 5. This is a common configuration used to fit impedance spectra from fuel cells [27]. The average error in the fitting of all spectra (twelve in total) was 0.0253, measured as the weighted sum of squares.

The equivalent circuit parameters obtained in ZView after the fitting of the spectra are compiled in Table 1.

The small relative variations of R1 (corresponding to the cell HFR) are also observed in Table 1, which is consistent with the observations analysed in Section 3.3. It is also observed that R2 (related to the electrochemical process resistance) is decreasing when current is increased, and W-R (related to the diffusion or mass transport process resistance) is increasing when current is increased due to mass transport limitations. Both trends are also well known in the literature [15–19,23]. Overall, the cell ohmic resistance is contributing with a weight of 20–30% to the total resistance. The electrochemical or activation polarization resistance is contributing with a weight of 20–50% (with higher contribution at lower current densities), and the mass transport of concentration polarization resistance is contributing with a weight of 20–60% (with higher contribution at higher current densities).

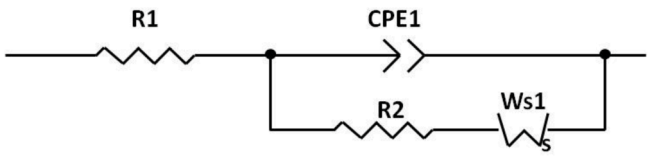

Fig. 5. Equivalent circuit used for the fitting of the impedance spectra.

Based on the parameters in Table 1, the sum of the resistances was determined, as R1 + R2 + W-R. R1 is corresponding to the ohmic resistance or HFR, R2 is corresponding to the resistance of the electrochemical reaction (activation polarization), and W-R is corresponding to the resistance of the reactants diffusion (mass transport or concentration polarization), as in the work by Dhirde et al. [28]. The result of the sum of all resistances is presented in Table 2 (named as EIS/EC Resistances). The voltage drop associated to these resistances is also presented in Table 2, as well as the resulting hysteresis calculated as the voltage difference when comparing the values for the forward and backward curves.

The first observation is that for all cases, the total resistance determined from the parameters of the Equivalent Circuit (named as EIS/EC Resistances in Table 2) for the backward curve is less than for the forward curve, supporting the fact that all experimental polarization curves are presenting backward/decreasing current curves with higher voltages than the corresponding forward/increasing current curves.

The voltage difference calculated and presented in Table 2 for each dwell time and each value of the current (EC Hysteresis in Table 2) was compared against the actual hysteresis measured in the polarization curves (as cell voltage backward current – cell voltage forward current). This was carried out in order to determine whether the hysteresis voltage differences calculated based on the fitting of the equivalent circuits (Table 2) are properly comparable to the real voltage differences measured in the polarization curves (Fig. 2). The results are presented in Fig. 6 for all cases measured.

It can be observed that the correspondence between experimental values of the cell hysteresis and the ones determined by the equivalent circuit is reasonably well, with the exception of high dwell times (1200 and 1800 s) at high current (50 A). In spite of the exceptions indicated, the agreement could be considered as acceptable enough in order to allow to further analyse the reasons why hysteresis is being observed, based on the values of the resistances determined from the equivalent circuits.

3.5. *Identification of the phenomena causing the cell hysteresis at each condition*

In Table 2, three additional data is calculated (ΔR1, ΔR2, and ΔW−R). Each value represents the variation of R1, R2 and W-R between the forward and the backward curves, for each dwell time and for each current. The absolute contribution of each polarization to the total resistance was discussed in the previous section, with a relatively constant contribution of ohmic resistance, an increasing contribution of mass concentration for higher current densities, and a decreasing contribution of activation polarization for higher current densities. These new values ΔR1, ΔR2, and ΔW−R in Table 2 are therefore representing the relative change in each polarization between the forward and the backward curve. This will thus provide information about the origin and cause of the cell voltage hysteresis observed in the polarization curves. It can be observed that variations in R1 can be neglected for all cases due to the very small differences between the forward and the backward curves, which is consistent with the observations and discussion provided in Section 3.3.

Interestingly, the relative changes of R2 and W-R (ΔR2 and ΔW-R in Table 2) are different depending on the particular case, but following a consistent trend: in all cases at 25 A, the relative contribution of ΔW-R (concentration polarization) is significantly higher than the relative contribution of ΔR2 (activation polarization). On the contrary, in all cases at 50 A, the relative contribution of ΔW-R (concentration polarization) is lower than the relative contribution of ΔR2 (activation polarization). The consequence of such observation is an interesting fact: first, it must be considered that the actual contribution of each polarization to the total resistance is as described above (i.e. higher contribution of mass concentration for higher current densities, and a lower

Table 1
Parameters of the equivalent circuit fitting the impedance spectra.

Experiment	R1 (Ω)	CPE-T	CPE-P	R2 (Ω)	W-R (Ω)	W-T	W-P
900 s 25A forward	0.00220	1.530	0.820	0.0034	0.0024	0.159	0.461
900 s 25A backward	0.00217	1.828	0.811	0.0033	0.0019	0.174	0.488
900 s 50A forward	0.00218	0.976	0.899	0.0022	0.0058	0.106	0.428
900 s 50A backward	0.00217	0.875	0.915	0.0020	0.0058	0.107	0.423
1200 s 25A forward	0.00220	1.690	0.807	0.0037	0.0028	0.163	0.469
1200 s 25A backward	0.00220	1.989	0.798	0.0035	0.0019	0.167	0.513
1200 s 50A forward	0.00220	0.864	0.916	0.0020	0.0068	0.112	0.411
1200 s 50A backward	0.00220	0.801	0.927	0.0019	0.0064	0.113	0.412
1800 s 25A forward	0.00209	1.724	0.809	0.0036	0.0023	0.147	0.489
1800 s 25A backward	0.00204	2.438	0.778	0.0036	0.0014	0.146	0.563
1800 s 50A forward	0.00206	1.578	0.849	0.0027	0.0046	0.088	0.464
1800 s 50A backward	0.00207	1.549	0.858	0.0025	0.0044	0.088	0.461

Table 2
Resistance obtained from the equivalent circuits for the different experimental tests, hysteresis calculated out of the resistances, and relative contribution of each polarization.

Experiment	EIS/EC Resistances (ohm)	Voltage drop (V)	EC Hysteresis (V)	ΔR1 (%)	ΔR2 (%)	ΔW-R (%)
900 s 25A forward	0.0080	0.200	0.0156	1.2	3.5	20.3
900 s 25A backward	0.0074	0.184				
900 s 50A forward	0.0102	0.510	0.0143	0.5	11.4	0. 4
900 s 50A backward	0.0099	0.496				
1200 s 25A forward	0.0087	0.217	0.0255	0.0	3.8	31.3
1200 s 25A backward	0.0077	0.192				
1200 s 50A forward	0.0110	0.552	0.0272	0.0	7.6	5.7
1200 s 50A backward	0.0105	0.525				
1800 s 25A forward	0.0080	0.201	0.0241	2.6	1.6	37.1
1800 s 25A backward	0.0071	0.176				
1800 s 50A forward	0.0094	0.469	0.0245	-0.5	9.9	5.0
1800 s 50A backward	0.0089	0.444				

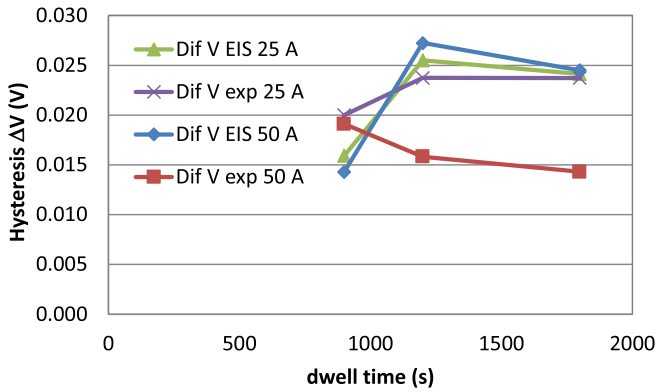

Fig. 6. Experimental cell voltage hysteresis (exp) and the corresponding cell voltage differences determined from the resistances of the equivalent circuit.

contribution of activation polarization for higher current densities, as observed in Fig. 4 and Table 1). But the data in Table 2 reveals that the cause of the cell voltage hysteresis is actually dominated by the variations in the concentration polarization at low current densities, and by the variations in the activation polarization at high current densities.

4. Discussion on the influence of dwell times on cell hysteresis

In Table 2, the resistance of the cell for each dwell time experiment is shown in column "EIS/EC Resistances". Fig. 6 represented the experimental cell voltage hysteresis together with the corresponding cell voltage differences determined from the resistances of the equivalent circuit, which is actually the hysteresis predicted by the Equivalent Circuit. It was determined that the correspondence between experimental values of the cell hysteresis and the ones determined by the Equivalent Circuit was reasonably well, with the exception of two points corresponding to high dwell times (1200 and 1800 s) at high current (50 A). Once the influence of the dwell times on the cell hysteresis was experimentally assessed (Fig. 1), it is reasonable to try determining the origin of such influence by analysing the information provided by the EIS experiments and the Equivalent Circuit. Table 3 presents the complete set of data for this analysis.

It was already observed in the experimental results that at 25 A the hysteresis is increasing when dwell time is incremented from 900 to 1200 s, and then remains constant for the 1800 s dwell time experiment. The difference in the values of the total resistance obtained in the EIS/Equivalent Circuit data (second column in Table 2) presents a consequent trend, with higher resistance differences obtained when hysteresis is higher. It was already discussed in Section 3.5 that at 25 A, the origin of the cell voltage hysteresis is mostly based on the differences or variations in the mass concentration polarization. This can be again observed in Table 3, where the values of the forward – backward W-R term are dominating the contribution to the total cell resistance difference. Analysing the data, it can be determined that the reason why cell voltage hysteresis for 900 s dwell time is lower than for 1200 or 1800 s is precisely the fact that the total cell resistance at 900 s dwell time is smaller, and this is mostly caused by the smaller values of the mass transport or concentration resistance. This is meaning that longer dwell times are causing an increase in the mass transport resistance and therefore a higher cell voltage hysteresis.

A similar analysis could be carry out for the case with 50 A, however with a minor degree of confidence as the difference in the behaviour between experimental hysteresis and EIS/EC hysteresis for longer dwell times at this higher current are avoiding an accurate analysis and conclusion.

5. Conclusions

The voltage hysteresis observed in fuel cells when the polarization curve is performed in forward direction with increasing current densities and then in backward direction with decreasing current densities was investigated in this work. The extent of the cell voltage hysteresis and the origins causing this effect are investigated by performing experimental polarization curves with different dwell times, for a 50 cm^2 PEM

Table 3
Resistance difference (forward curve - backward curve, denoted as FW-BW) obtained from the equivalent circuits for the different experimental tests, and contribution of each polarization.

dwell time / current	EIS/EC total resistance difference (FW - BW) (mOhm)	Δ R1 (FW-BW) (mOhm)	Δ R2(FW-BW) (mOhm)	Δ W-R(FW-BW) (mOhm)	Hysteresis EIS/EC (V)	Hysteresis experiment (V)
900 s / 25 A	0.6	0.026	0.120	0.491	0.016	0.020
1200 s / 25 A	1.0	0.000	0.140	0.880	0.026	0.024
1800 s / 25 A	1.0	0.055	0.060	0.850	0.024	0.024
900 s / 50 A	0.3	0.010	0.250	0.026	0.014	0.019
1200 s / 50 A	0.5	0.000	0.155	0.390	0.027	0.016
1800 s / 50 A	0.5	-0.010	0.270	0.230	0.025	0.014

fuel cell. Electrochemical Impedance Spectroscopy measurements were carried out in order to determine the relative contributions of the different polarizations (ohmic, activation, and mass transport or concentration polarization). Equivalent circuits were obtained from the experimental impedance spectra, where the interpretation of the circuit parameters enabled the analysis of the origin and the extent of the cell voltage hysteresis. It was identified that the cause of the cell voltage hysteresis is actually dominated by the variations in the concentration polarization (ΔR2 in Table 2) at low current densities, and by the variations in the activation polarization (ΔW-R in Table 2) at high current densities, while the relative contribution to the total polarization of the cell is the opposite, with concentration polarization dominating at high current densities and activation polarization dominating at low current densities. The cell ohmic resistance (and consequently the membrane hydration) presents no effect on the cell voltage hysteresis. The effect of the dwell time in the cell voltage hysteresis (with values ranging from 15 to 25 mV) presents a mixed trend. The hysteresis initially decreases when increasing dwell times from 120 to 600 s, but then starts to increase until 900 s dwell time, and then remains almost constant with minor variations until 1800 s.

CRediT authorship contribution statement

Alfredo Iranzo: Conceptualization, Data curation, Formal analysis, Funding acquisition, Investigation, Methodology, Project administration, Supervision, Writing – original draft, Writing – review & editing. **Sergio J. Navas:** Data curation, Formal analysis, Investigation, Methodology, Software, Visualization, Writing – original draft, Writing – review & editing. **Javier Pino:** Investigation, Project administration, Resources, Supervision. **Numa A. Althubiti:** Funding acquisition, Project administration, Resources. **Mohamed R. Berber:** Funding acquisition, Investigation, Methodology, Project administration, Supervision, Resources, Writing – review & editing.

Declaration of Competing Interest

The authors declare that they have no known competing financial interests or personal relationships that could have appeared to influence the work reported in this paper.

Acknowledgments

The authors extend their appreciation to the Deputyship for Research & Innovation, Ministry of Education in Saudi Arabia for co-funding this research work through the Project No. “375213500”. This work has been developed thanks to the funding of the Spanish Ministry of Science, Innovation and Universities (Grant ENE2017-91159-EXP and PID2019-104441RB-I00), the Spanish Ministry of Economy and Competitiveness (Grant UNSE15-CE2962), all projects funded by AEI/FEDER UE, and the Consejería de Economía, Conocimiento, Empresas y Universidad, PAIDI 2020 program by Junta de Andalucía (PY20 RE026 AICIA), co-funded with ERDF funds. The authors also would like to extend their sincere appreciation to the central laboratory at Jouf University for the support of this study.

References

[1] F. Barbir, PEM Fuel Cells: Theory and Practice, 1st ed., Elsevier Academic, 2005.
[2] J. Hamelin, K. Agbossou, A. Laperriere, F. Laurencelle, TK. Bose, Dynamic behavior of a PEM fuel cell stack for stationary applications, Int. J. Hydrog. Energy 26 (2001) 625–629.
[3] S. Kim, S. Shimpalee, JW. VanZee, The effect of stoichiometry on dynamic behavior of a proton exchange membrane fuel cell (PEMFC) during load change, J. Power Sources 135 (2004) 110–121.
[4] H. Yu, C. Ziegler, Transient behavior of a proton exchange membrane fuel cell under dry operation, J. Electrochem. Soc. 153 (2006) A570–A575.
[5] J. Mitzel, E. Gülzow, A. Kabza, J. Hunger, S.S. Araya, P. Piela, I. Alecha, G. Tsotridis, Identification of critical parameters for PEMFC stack performance characterization and control strategies for reliable and comparable stack benchmarking, Int. J. Hydrog. Energy 41 (2016) 21415–21426.
[6] G. Tsotridis, A. Pilenga, G. DeMarco, T. Malkow, EU Harmonised Test Protocols for PEMFC MEA Testing in Single cell Configuration for Automotive Applications, Publications Office of the European Union, 2015, https://doi.org/10.2790/342959. ISBN: 978-92-79-54133-9 (print),978-92-79-54132-2 (PDF)print10.2790/54653 (online).
[7] T. Bednarek, G. Tsotridis, Assessment of the electrochemical characteristics of a polymer electrolyte membrane in a reference single fuel cell testing hardware, J. Power Sources 473 (2020), 228319.
[8] J. Hou, A study on polarization hysteresis in PEM fuel cells by galvanostatic step sweep, Int. J. Hydrog. Energy 36 (2011) 7199–7206.
[9] C.Y. Wang, Fundamental models for fuel cell engineering, Chem. Rev. 104 (10) (2004) 4727–4765.
[10] A. Iranzo, M. Muñoz, F.J Pino, F. Rosa, Non-dimensional analysis of PEM fuel cell phenomena by means of AC impedance measurements, J. Power Sources 196 (2011) 4264–4269.
[11] A. Iranzo, P. Boillat, CFD simulation of the transient gas transport in a PEM fuel cell cathode during AC impedance testing considering liquid water effects, Energy 158 (2018) 449–457.
[12] A. Iranzo, A. Salva, P. Boillat, J. Biesdorf, E. Tapia, F. Rosa, Water build-up and evolution during the start-up of a PEMFC: visualization by means of neutron imaging, Int. J. Hydrog. Energy 42 (19) (2017) 13839–13849.
[13] K.C. Neyerlin, W. Gu, J. Jorne, H.A. Gasteiger, Determination of catalyst unique parameters for the oxygen reduction reaction in a PEMFC, J. Electrochem. Soc. 153 (2006) A1955–A1963.
[14] N. Fouquet, C. Doulet, C. Nouillant, G. Dauphin-Tanguy, B. Ould-Bouamama, Model based PEM fuel cell state-of-health monitoring via ac impedance measurements, J. Power Sources 159 (2006) 905–913.
[15] J. Wu, X.Z. Yuan, H. Wang, M. Blanco, J. Zhang, Diagnostic tools in PEM fuel cell research: part I electrochemical techniques, I Int. J. Hydrog. Energy 33 (2008) 1735–1746.
[16] S.M.R. Niya, M. Hoorfar, Study of proton exchange membrane fuel cells using electrochemical impedance spectroscopy technique – a review, J. Power Sources 240 (2013) 281–293.
[17] Z. Tang, Q.A. Huang, Y.J. Wang, F. Zhang, W. Li, A. Li, L. Zhang, J. Zhang, Recent progress in the use of electrochemical impedance spectroscopy for the measurement, monitoring, diagnosis and optimization of proton exchange membrane fuel cell performance, J. Power Sources 468 (2020), 228361.
[18] X. Yuan, H. Wang, J. ColinSun, J. Zhang, AC impedance technique in PEM fuel cell diagnosis-A review, Int. J. Hydrog. Energy 32 (2007) 4365–4380.
[19] A. Iranzo, M. Muñoz, E. López, J. Pino, F. Rosa, Experimental fuel cell performance analysis under different operating conditions and bipolar plate designs, Int. J. Hydrog. Energy 35 (2010) 11437–11447.
[20] W. Alexandra, S. Stefan, G. Samuele, M.A. Danzer, Z. Roswitha, Distribution of relaxation times analysis of high-temperature PEM fuel cell impedance spectra, Electrochim. Acta (2017) 391–398, 23010.
[21] H. Marcel, W. André, I.T. Ellen, Advanced impedance study of polymer electrolyte membrane single cells by means of distribution of relaxation times, J Power Sources 402 (31) (2018) 24–33.
[22] H. Marcel, W. André, I.T. Ellen, Impedance modelling of porous electrode structures in polymer electrolyte membrane fuel cells, J. Power Sources 444 (31) (2019), 227279.
[23] A. Iranzo, S.J. Navas, F. Rosa, M.R. Berber, Determination of time constants of diffusion and electrochemical processes in polymer electrolyte membrane fuel cells, Energy 221 (2021), 119833.

[24] S.M. RezaeiNiya, R.K. Phillips, M. Hoorfar, Process modeling of the impedance characteristics of proton exchange membrane fuel cells, Electrochim. Acta 191 (2016) 594–605.
[25] M. Mench, Fuel cell engines (2008).
[26] ZView software. Scribner Associates, Inc. 150 East Connecticut Avenue. Southern Pines, NC 28387.
[27] X.Z. Yuan, S. Chaojie, W. Haijiang, Z. Jiujun, Electrochemical Impedance Spectroscopy in PEM Fuel Cells: Fundamentals and Applications, Springer, London, 2010, p. 87.
[28] A.M. Dhirde, N.V. Dale, H. Salehfar, M.D. Mann, T.H. Han, Equivalent electric circuit modeling and performance analysis of a PEM fuel cell stack using impedance spectroscopy, IEEE Trans. Energy Convers. 25 (2010) 778–786.